

MOS-Attack: A Scalable Multi-objective Adversarial Attack Framework

Ping Guo^{1,2}, Cheng Gong^{1,2}, Xi Lin^{1,2}, Fei Liu^{1,2}, Zhichao Lu^{1,2}, Qingfu Zhang^{1,2*}, Zhenkun Wang³
¹City University of Hong Kong; ²CityU Shenzhen Research Institute;
³Southern University of Science and Technology

Abstract

Crafting adversarial examples is crucial for evaluating and enhancing the robustness of Deep Neural Networks (DNNs), presenting a challenge equivalent to maximizing a non-differentiable 0-1 loss function. However, existing single objective methods, namely adversarial attacks focus on a surrogate loss function, do not fully harness the benefits of engaging multiple loss functions, as a result of insufficient understanding of their synergistic and conflicting nature. To overcome these limitations, we propose the Multi-Objective Set-based Attack (MOS Attack), a novel adversarial attack framework leveraging multiple loss functions and automatically uncovering their interrelations. The MOS Attack adopts a set-based multi-objective optimization strategy, enabling the incorporation of numerous loss functions without additional parameters. It also automatically mines synergistic patterns among various losses, facilitating the generation of potent adversarial attacks with fewer objectives. Extensive experiments have shown that our MOS Attack outperforms single-objective attacks. Furthermore, by harnessing the identified synergistic patterns, MOS Attack continues to show superior results with a reduced number of loss functions.

1. Introduction

Deep neural network (DNN) models have significantly advanced the field of computer vision [15, 26, 28, 38], yet they are vulnerable to adversarial examples [20, 43]. Such examples are inputs that have been subtly modified to cause misclassification, potentially leading to catastrophic consequences in real-world scenarios [7, 16, 19]. Consequently, the development of sophisticated adversarial attack algorithms is crucial for evaluating and enhancing the robustness of these models [11, 34, 52]. However, devising these algorithms presents inherent challenges due to the non-differentiable nature of the original optimization problem, necessitating the use of surrogate loss functions [21] to fa-

cilitate gradient-based adversarial attacks [11, 20, 34].

The metric for measuring misclassification is the non-differentiable 0-1 loss function, which surrogate loss functions endeavor to approximate [30]. Adversarial attacks are designed to generate a perturbation δ that causes the misclassification of an input \mathbf{x} with its corresponding label \mathbf{y} . This can be formulated as [21, 34]:

$$\max_{\delta \in \mathcal{B}} L_{0-1}(\mathbf{h}_{\theta}(\mathbf{x} + \delta), \mathbf{y}), \quad (1)$$

where \mathbf{h}_{θ} represents the DNN model parameterized by θ , L_{0-1} denotes the 0-1 loss function, and \mathcal{B} is the set of allowable perturbations.

Considering the computational intractability of the problem in Equation (1) [3], contemporary research commonly employs a differentiable surrogate loss function in place of the 0-1 loss function. This approach enables the utilization of gradient-based optimization techniques to address the resultant surrogate optimization problem. It has propelled considerable progress in gradient-based algorithms, including the Fast Gradient Sign Method (FGSM) [20], Projected Gradient Descent (PGD) [34], and Carlini & Wagner (C&W) attack [8]. Notably, the versatility of the PGD attack has increased with the adoption of diverse surrogate loss functions (APGD-CE, APGD-DLR) [41] and the integration of sophisticated optimization techniques (ACG) [51]. These developments have given rise to more sophisticated adversarial methods.

While single-objective attacks have attracted considerable attention, there is an emerging trend towards integrating multiple loss functions to bolster the attack's efficacy. Some early endeavors include using multiple targeted loss functions to guide untargeted attack [21] and the strategic alternation of loss functions in the attack process[2]. Furthermore, the adoption of diverse surrogate loss functions such as GAMA [41], BCE [46], and DLR [11] has been instrumental in advancing adversarial attacks.

Despite the potential advantages for incorporating multiple loss functions, direct optimization with a vast array of adversarial examples is inefficient. Moreover, the methodology for targeting suitable loss functions to mount effective adversarial attacks is lacking. Therefore, it is imperative

*Corresponding author: qingfu.zhang@cityu.edu.hk

to develop a scalable framework that can efficiently coordinate multiple surrogate loss functions, concentrate on a limited subset, and reduce the number of adversarial examples needed for optimization.

To bridge this knowledge gap, we introduce the Multi-Objective Set-based Attack (MOS Attack), a novel framework for conducting multi-objective adversarial attacks and investigating the interactions among various surrogate loss functions. Our framework notably offers: 1) a scalable, parameter-free template for executing multi-objective adversarial attacks, and 2) automated method for the discovery of synergistic loss patterns. The MOS Attack employs a suite of surrogate loss functions and initiates an adaptable number of adversarial examples, thereby defining a smooth set-based optimization problem. Subsequently, single-objective gradient-based optimization techniques, which require only minimal adjustments, can efficiently address this problem. Following the optimization phase, an automated analysis identifies synergistic patterns within the adversarial examples. These patterns enable the construction of powerful multi-objective adversarial attacks that require fewer objectives, allowing a more efficient allocation of computational resources to each objective.

We have implemented our approach using four widely recognized surrogate loss functions as outlined in previous research [41, 46], as well as four additional functions identified through extensive loss function searches [30, 50]. The resulting MOS-8¹ Attack has proven highly effective through extensive experimentation on the CIFAR-10 [28] and ImageNet [15] datasets, outperforming state-of-the-art methods that leverage advanced gradient-based optimization or eight distinct single-objective attacks for each surrogate loss. Moreover, by examining the synergistic patterns uncovered by MOS-8 Attack, we have developed a tri-objective attack, MOS-3*, which has also shown superior performance.

Our contributions can be summarized as follows:

- We introduce the first multi-objective adversarial attack framework, the MOS Attack, which tackles the challenge of generating adversarial examples with multiple loss functions. This framework is parameter-free and readily extensible with new loss functions.
- Our framework also offers an automated method for identifying synergistic patterns among loss functions, which can be used to construct powerful multi-objective attacks with fewer objectives, facilitating a more efficient allocation of computational resources.
- We have implemented our framework with 8 loss functions to form the MOS-8 Attack, which has been extensively tested on CIFAR-10 and ImageNet datasets. Ad-

¹We use MOS-8 Attack to denote MOS Attack implemented with 8 loss functions, MOS-3* to denote the attack implemented with three selected loss functions.

ditionally, synergistic analysis over these 8 loss functions has been conducted to provide insights regarding their interactions and led to the development of a powerful tri-objective attack, MOS-3*.

2. Background

Adversarial attacks encompass methods that create adversarial examples, which are used to assess and enhance model robustness [11, 34]. A white-box threat model is often considered for evaluating adversarial robustness, where the adversary has full access to the model’s architecture, parameters, and gradients. While white-box existing strategies mainly focus on one surrogate loss function [1, 18, 25, 51], a recent trend is the integration of multiple loss functions into the attack paradigm [5, 14, 33, 42, 44].

Single-Objective Attacks. White-box attack methodologies typically employ a singular surrogate loss function, focusing on optimization to craft adversarial examples. Established strategies include the FGSM [20], C&W attack [8], and PGD attack [34]. Croce *et al.* proposed a novel parameter-free approach, Auto-PGD (APGD) attack, utilizing both Cross Entropy (CE) and the Difference of Logits Ratio (DLR) loss functions. These were subsequently incorporated into the AutoAttack framework as APGD-CE and APGD-DLR [11]. Expanding upon this, Yamamura *et al.* enhanced APGD with conjugate gradient techniques, resulting in the creation of the powerful Auto Conjugate Gradient (ACG) attack [51].

Multi-Objective Attacks. Recent advancements in adversarial research have involved the integration of multiple surrogate loss functions into the attack framework. Goyal *et al.* introduced multiple targeted losses to enhance untargeted PGD attacks [21]. Further, work by Nikolaos *et al.* established that the strategic variation of surrogate loss functions considerably improve adversarial attack performance [2]. However, these studies typically lack a systematic approach and a solid theoretical underpinning for managing multiple losses.

Concurrently, researchers have expanded the adversarial attack framework by introducing other types of objectives. Williams *et al.* investigated the inclusion of additional norm constraints [48], while Guo *et al.* and Liu *et al.* have investigated the trade-off between perturbation intensity and confidence measures [24, 33]. These efforts have contributed to the development of more diversified attack methodologies.

Our approach represents the first attempt to systematically incorporate multiple loss functions into adversarial attacks and optimize the corresponding multi-objective optimization problem using a minimal set of examples via smooth set-based optimization techniques.

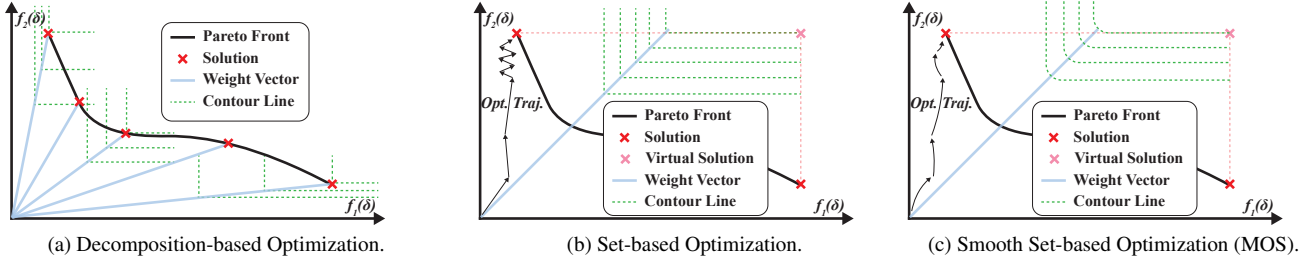


Figure 1. Comparison of different optimization methods for conducting multi-objective adversarial attacks.

3. Multi-Objective Set-based Attack

In this section, we propose the problem formulation of the smooth set-based approach for multi-objective adversarial attacks. We begin by defining the multi-objective adversarial attack, which employs multiple surrogate loss functions, as a multi-objective optimization problem. Subsequently, we introduce the decomposed subproblems and identify three optimization challenges. Finally, we propose the formulation of the smooth set-based optimization problem as a solution to the challenges posed by the multi-objective nature of adversarial attacks.

3.1. Multi-Objective Adversarial Attack

This study seeks to simultaneously optimize multiple surrogate loss functions, rather than relying on a singular loss function, to craft adversarial examples. Given m loss functions L_1, \dots, L_m , we define a multi-objective optimization problem as follows:

$$\begin{aligned} \max_{\delta \in \mathcal{B}} \mathbf{f}(\delta) &= (f_1(\delta), \dots, f_m(\delta)), \\ f_i(\delta) &= L_i(\mathbf{h}_\theta(\mathbf{x} + \delta), y), \forall i \in \{1, \dots, m\}. \end{aligned} \quad (2)$$

The notation remains consistent with the single-objective scenario as depicted in Equation (1). Furthermore, this paper adopts the extensively utilized ℓ_∞ -ball as the constraint set for perturbations, denoted by $\mathcal{B} = \{\delta : \|\delta\|_\infty \leq \epsilon\}$.

Examples with higher values across multiple surrogate loss functions are more susceptible to misclassification by the model. In existing literature, this statement is supported by frequent misclassifications of adversarial examples with high values on singular loss functions [11, 34, 51].

Nevertheless, since there is often no single solution that maximizes all the loss functions simultaneously, a set of best trade-off solutions becomes necessary. This set of solutions is called the Pareto set, and the corresponding values of the objective functions are called the Pareto front. A formal description of Pareto optimality is delineated below:

Definition 3.1 (Pareto Optimal). A solution δ^* is Pareto optimal if there is no other solution δ such that $f_i(\delta) \geq f_i(\delta^*)$ for all $i \in \{1, \dots, m\}$ and $f_i(\delta) > f_i(\delta^*)$ for at least one $i \in \{1, \dots, m\}$.

Definition 3.2 (Pareto Set and Pareto Front). The Pareto set is the set of all Pareto optimal solutions, and the Pareto front is the set of all the values of the objective functions at the Pareto optimal solutions.

3.2. Decomposition-Based Optimization

In this research, we employ the Tchebycheff decomposition to transform the multi-objective problem into a suite of single-objective subproblems. Contrary to the linear scalarization method, the Tchebycheff approach is capable of targeting any location on the Pareto front. This is well-recognized in the discipline of multi-objective optimization [13, 35, 53]. By adopting this method, given K weight vectors $\mathbf{w}_1, \dots, \mathbf{w}_K$, the k -th decomposed subproblem is defined as follows:

$$\max_{\delta \in \mathcal{B}} g_k(\delta | \mathbf{w}_k) = \min_i w_{ki} |f_i(\delta) - z_i^*|, \quad (3)$$

where w_{ki} is the i -th element of the k -th weight vector, and z_i^* denotes the ideal value for the i -th objective. Upon solving these subproblems, a set of solutions correlated with the weight vectors is obtained. This set can approximate the Pareto set, as illustrated in Figure 1a.

The Tchebycheff method is instrumental in identifying both convex and non-convex parts of the Pareto front with vertical contour lines [45], as demonstrated in Figure 1a. Nonetheless, it presents three challenges in optimization:

- **Complexity:** Accurate approximation of the Pareto front necessitates multiple points, exceeding the number of objectives ($> m$).
- **Ambiguity:** The selection of appropriate weight vectors is challenging.
- **Non-differentiability:** The function g_k contains non-differentiable points.

3.3. Smooth Set-based Optimization

To address the challenges associated with Tchebycheff decomposition, we propose a formulation that leverages a smooth set-based optimization approach. The primary issue is the number of adversarial examples needed to maximize the surrogate loss functions. We tackle this by deliberately selecting a set of K adversarial examples, with

$K < m$. Additionally, we default the weight vector to an all-ones configuration to eliminate the ambiguity in selecting the weight vector. Lastly, we smooth the optimization problem to circumvent non-differentiability issues.

Set-based Optimization Suppose we have a set of K adversarial examples $\Delta = \{\delta_1, \dots, \delta_K\}$ to accommodate multiple objectives and one weight vector \mathbf{w} for specifying the contour lines. The set-based optimization problem can be formulated as:

$$\max_{\Delta} g(\Delta|\mathbf{w}) = \min_i w_i \left| \max_{k_i} f_i(\delta_{k_i}) - z_i^* \right|, \quad (4)$$

where w_i is the i -th element of the weight vector, and z_i^* is the optimal value of the i -th objective function.

A Geometric Interpretation. The inner maximization problem as formulated in Equation (4) allows each perturbation vector, $\delta \in \Delta$, to impart its dimensionality upon the objective function. We conceive a 'virtual adversarial example' as a combination of the most advantageous dimensional attributes of adversarial examples. The essence of the set-based optimization procedure lies in pushing this virtual adversarial example towards extreme points along the contour lines, as depicted in Figure 1b.

We investigate the relationship between the number of adversarial examples K and the number of loss functions m . Specifically:

- $K < m$: A smaller number of adversarial examples are utilized to address a multitude of objectives. This approach enables optimization of the functions using reduced resources. In the extreme scenario where $K = 1$, a single solution must fulfill all objectives.
- $K = m$: there exists a theoretical optimal solution comprising the individual optimal adversarial examples for each objective function. Through proper optimization, this ideal state may be achieved.

So far, the first two challenges of decomposition-based optimization have been addressed by the set-based optimization problem. However, the third challenge remains unresolved. This can lead to oscillation in the optimization process, as illustrated in Figure 1b. Therefore, we need to design a smooth approximation of the set-based optimization problem.

Smooth Set-based Optimization To smooth the above optimization problem, we need to take advantage of smooth max and smooth min operators [6, 31, 32].

$$\begin{aligned} \max \{x_1, \dots, x_m\} &\approx \mu \log \left(\sum_{i=1}^m e^{x_i/\mu} \right), \\ \min \{x_1, \dots, x_m\} &\approx -\mu \log \left(\sum_{i=1}^m e^{-x_i/\mu} \right), \end{aligned} \quad (5)$$

where μ is a smoothing parameter. A proof of the above approximation can be found in [6].

Using the above operators, the objective function in Equation (4) can be approximated as:

$$\begin{aligned} g(\Delta|\mathbf{w}) &= \min_i w_i \left| \max_{k_i} f_j(\delta_{k_i}) - z_i^* \right|, \\ &\approx -\mu \log \left(\sum_i^m e^{-(w_i |\mu \log(\sum_{k=1}^K e^{f_i(\delta_k)/\mu}) - z_i^*)/\mu} \right). \end{aligned} \quad (6)$$

Furthermore, if we consider $z_i^* = 0$ and a uniform weight vector with $w_i = w_j, \forall i, j$, we can get our final optimization problem as:

$$\max_{\Delta} g(\Delta) = -\mu \log \left(\sum_i^m \left(\sum_{k=1}^K e^{f_i(\delta_k)/\mu} \right)^{-1} \right). \quad (7)$$

The above formulation eases the optimization process and avoids oscillations in the optimization process, which is analyzed in the multi-objective literature [32]. We illustrate the smoothed set-based optimization problem along with a possible optimization trajectory in Figure 1c.

4. Methodology

4.1. MOS Attack: Implementation by APGD

By formulating a smooth set-based optimization problem, we can now apply gradient-based optimization algorithms for its efficient resolution. Within the domain of adversarial attacks, our framework incorporates the well-known APGD algorithm [11]. In this section, we provide a detailed explanation of our attack, as outlined in Algorithm 1.

Initialization. The initialization process involves specifying the input parameters and determining the initial adversarial examples. We follow a procedure similar to that used in the APGD. However, our approach take as input 1) a set of adversarial examples Δ , and 2) an objective function $g(\Delta)$ defined in Equation (7).

Momentum-based Update Rule. We adopt the same momentum-based update rule as in APGD, which is considered to be stable and efficient. The details are delineated in lines 9 and 10 of Algorithm 1. Our modification addresses the optimization of a set of adversarial examples rather than a single example. Therefore, we have adjusted the update rule to: 1) optimize \mathbf{X} and Δ concurrently, and 2) implement a set-based projection operator.

Optimization Representation. Considering our function g incorporates Δ and subsequent projection requires \mathbf{X} 's range, concurrent optimization of both is essential. Notably, the statement in line 9 consistently applies because $\nabla_{\mathbf{X}} g(\Delta) = \nabla_{\Delta} g(\Delta)$, with $\mathbf{X} = \Delta + \mathbf{x}$.

Table 1. The loss function utilized for implementing our attack.

ID	Loss Function	Formula
0	Cross Entropy Loss [8, 20, 29, 34, 43]	$-\mathbf{h}_y(\mathbf{x}) + \log(\sum_{i=1}^K e^{h_i(\mathbf{x})})$
1	Marginal Loss [8, 10, 11, 21, 41]	$-\mathbf{h}_y(\mathbf{x}) + \max_{j \neq y} \mathbf{h}_j(\mathbf{x})$
2	Difference of Logits Ratio [10]	$(-\mathbf{h}_y(\mathbf{x}) + \max_{j \neq y} \mathbf{h}_j(\mathbf{x})) / (\mathbf{h}_{\pi_1}(\mathbf{x}) - \mathbf{h}_{\pi_3}(\mathbf{x}))$
3	Boosted Cross-Entropy Loss [46]	$-\log \mathbf{p}_y(\mathbf{x}) - \log(1 - \max_{j \neq y} \mathbf{p}_j(\mathbf{x}))$
4	Searched Loss 1 [50]	$\sum_i \exp(10\mathbf{p} / \max_j \mathbf{p}_j)$
5	Searched Loss 2 [50]	$\exp(-\max(\text{softmax}(\mathbf{h} + 2\text{softmax}(5\mathbf{h})))$
6	Searched Loss 3 [50]	$\text{softmax}(-\text{softmax}(2 \exp(\mathbf{h} \mathbf{h})))(\text{softmax}(2\mathbf{h}) + 2\mathbf{y}_{\text{one-hot}})$
7	Searched Loss 4 [50]	$(\text{softmax}(\text{softmax}(2\mathbf{h}) + \mathbf{h} - \mathbf{y}_{\text{one-hot}}) - \mathbf{y}_{\text{one-hot}})^2$

Table 2. The notations used in the loss functions.

Notation	Description
\mathbf{x}	The adversarial example.
\mathbf{h}	The vector of logits.
\mathbf{h}_y	The logit corresponding to the true class.
\mathbf{h}_j	The logit corresponding to the j -th class.
\mathbf{h}_{π_i}	The i -th highest logit.
\mathbf{p}_y	The probability corresponding to the true class.
\mathbf{p}_j	The probability corresponding to the j -th class.
$\mathbf{y}_{\text{one-hot}}$	The one-hot vector corresponding to the true class.

Algorithm 1 MOS Attack

```

1: Input:  $g, \mathcal{B}, \Delta^{(0)}, \eta, N_{\text{iter}}, W = \{w_0, \dots, w_n\}$ 
2: Output:  $\Delta_{\text{adv}}$ 
3:  $\mathbf{X}^{(0)} \leftarrow \mathbf{x} + \Delta^{(0)}$ 
4:  $\mathbf{X}^{(1)} \leftarrow P_{\mathcal{B}}(\mathbf{X}^{(0)} + \eta \nabla g(\Delta^{(0)}))$ 
5:  $\Delta^{(1)} \leftarrow \mathbf{X}^{(1)} - \mathbf{x}$ 
6:  $g_{\max} \leftarrow \max\{g(\Delta^{(0)}), g(\Delta^{(1)})\}$ 
7:  $\mathbf{X}_{\max} \leftarrow \mathbf{X}^{(0)}$  if  $g_{\max} \equiv g(\Delta^{(0)})$  else  $\mathbf{X}_{\max} \leftarrow \mathbf{X}^{(1)}$ 
8: for  $k = 1$  to  $N_{\text{iter}} - 1$  do
9:    $\mathbf{Z}^{(k+1)} \leftarrow P_{\mathcal{B}}(\mathbf{X}^{(k)} + \eta \nabla g(\Delta^{(k)}))$ 
10:   $\mathbf{X}^{(k+1)} \leftarrow P_{\mathcal{B}}(\mathbf{X}^{(k)} + \alpha(\mathbf{Z}^{(k+1)} - \mathbf{X}^{(k)}) + (1 - \alpha)(\mathbf{X}^{(k)} - \mathbf{X}^{(k+1)}))$ 
11:   $\Delta^{(k+1)} \leftarrow \mathbf{X}^{(k+1)} - \mathbf{x}$ 
12:  if  $g(\Delta^{(k+1)}) > g_{\max}$  then
13:     $\mathbf{X}_{\max} \leftarrow \mathbf{X}^{(k+1)}$  and  $g_{\max} \leftarrow g(\Delta^{(k+1)})$ 
14:  end if
15:  if  $k \in W$  then
16:    if Condition 1 or Condition 2 then
17:       $\eta \leftarrow \eta/2$  and  $\mathbf{X}^{(k+1)} \leftarrow \mathbf{X}_{\max}$  and  $\Delta^{(k+1)} \leftarrow \mathbf{X}_{\max} - \mathbf{x}$ 
18:    end if
19:  end if
20: end for

```

Set-based Projection. A pivotal component in gradient-based adversarial methodologies is the projection operator, which constrains the adversarial examples within the defined perturbation bounds. In our context, the challenge entails projecting an ensemble of adversarial examples. This is executed by individually projecting each example within the allowable perturbation boundary.

Step Size Adjustment. We use the same step size control method in APGD. The initial step size η is set to 2ϵ , where ϵ is the perturbation budget. When the checkpoint is reached, the following two conditions are checked:

1. $N_{\text{inc}} < \rho(w_j - w_{j-1})$,
2. $\eta^{w_{j-1}} = \eta^{w_j}$ and $g_{\max}^{w_{j-1}} = g_{\max}^{w_j}$,

where $N_{\text{inc}} = \#\{i = w_{j-1}, \dots, w_j - 1 | g(\Delta^{(i+1)}) > g(\Delta^{(i)})\}$ and $g_{\max}^k = \max\{g(\Delta^{(i)}) | i = 1, \dots, k\}$.

4.2. Automated Synergistic Pattern Mining

Few solutions automatically maximize different loss functions in groups in smooth set-based optimization [31]. To mine these loss synergistic patterns, we propose an automated mining method. This method includes two steps: 1) determining the dominant examples that contribute to the loss maximization, and 2) determining the synergistic pattern of these dominant examples.

Determining Dominant Examples. With a set of K perturbations $\Delta = \{\delta_1, \dots, \delta_K\}$ from the MOS Attack, we aim to identify the dominant perturbations that maximize the loss functions. Formally, we want to find an index vector $\beta = [\beta_1, \dots, \beta_K]$, $\beta_i \in \{0, 1\}, \forall i$, for specifying a subset of perturbations $\Delta_{\beta} = \{\delta_i | \beta_i = 1\}$ that still maximize the loss functions.

We first perform min-max normalization on the loss functions $f_i(\delta_k), \forall i$, and then the above formulation can be rewritten as a bi-objective optimization problem:

$$\min_{\beta} \left(\sum_{i=1}^m \max_{k=1}^K \bar{f}_i(\delta_k) - \max_{k=1}^K \beta_k \bar{f}_i(\delta_k), \|\beta\|_0 \right), \quad (8)$$

where $\bar{f}_i(\delta_k)$ is the normalized loss function. The first term serves to minimize the optimization gap. The ℓ_0 norm, which is the number of non-zero elements in a vector, aims to minimize the number of selected examples.

Smooth Relaxation. Since the above problem is an NP-hard combinatorial optimization problem, we relax it by introducing a smooth relaxation. Specifically, we relax the first objective by incorporating smooth operators in Equation (5) and the second objective by replacing the ℓ_0 norm with the ℓ_1 norm. The relaxed problem is then:

$$\min_{\beta} \sum_{i=1}^m \mu \log \left(\frac{\sum_{k=1}^K e^{f_i(\delta_k)/\mu}}{\sum_{k=1}^K e^{\beta_k f_i(\delta_k)/\mu}} \right) + \lambda \|\beta\|_1, \quad (9)$$

s.t. $\beta \in [0, 1]^K$,

where λ controls the sparsity.

The above problem is smooth and fully differentiable, and we can solve it using gradient-based methods. After the above problem is solved, we can get the dominant example index β . Here, we set a threshold T to further make β binary.

Table 3. **Overall Results.** A comparative analysis of attack success rate among MOS-8 attacks with APGD-CE, ACG-CW, and APGD-All. For MOS-8 Attack, we record its K value, while for others it denoted the number of restarts. Notably, for APGD-All, we have documented the index of the surrogate loss functions corresponding to the highest attack success rate. The optimal outcome is highlighted in bold and marked with a grey background. The second-best performance is underscored for emphasis.

CIFAR-10 ($\epsilon = 8/255$)			Attack Success Rate						Diff.(5) MOS CE
			Single-Objective			Multi-Objective			
			APGD (1)	APGD (5)	ACG [†] (5)	All (1)*8	MOS-8 (1)	MOS-8 (5)	
ID	Paper	Architecture							
0	Rade <i>et al.</i> (2022) [36] (<i>ddpm</i>)	PreActResNet-18	39.17	39.28	42.65	42.78 (6)	42.59	<u>42.77</u>	+3.49
1	Rade <i>et al.</i> (2022) [36] (<i>extra</i>)	PreActResNet-18	38.55	38.72	42.12	<u>42.21</u> (6)	42.03	42.23	+3.51
2	Schwag <i>et al.</i> (2022) [40]	ResNet-18	41.57	41.76	44.79	44.16 (6)	43.79	<u>44.18</u>	+2.42
3	Chen <i>et al.</i> (2020) [9]	ResNet-50	45.80	45.95	48.28	48.04 (4)	48.09	48.14	+3.49
4	Gowal <i>et al.</i> (2020) [22]	WideResNet-28-10	34.31	34.46	36.90	36.96 (6)	36.77	<u>36.95</u>	+2.19
5	Wang <i>et al.</i> (2023) [47]	WideResNet-28-10	29.72	29.91	N/A	<u>32.44</u> (6)	32.25	32.49	+2.58
6	Rebuffi <i>et al.</i> (2021) [37]	WideResNet-28-10	35.97	36.15	38.80	<u>39.05</u> (6)	38.91	39.14	+2.99
7	Schwag <i>et al.</i> (2022) [40]	WideResNet-34-10	36.85	36.96	40.18	39.36 (5)	38.97	<u>39.38</u>	+2.43
8	Rade <i>et al.</i> (2022) [36]	WideResNet-34-10	34.29	34.45	36.83	36.97 (6)	36.69	<u>36.94</u>	+2.49
9	Gowal <i>et al.</i> (2021) [23]	WideResNet-70-16	31.43	31.62	33.04	<u>33.50</u> (5)	33.33	33.51	+1.89
10	Gowal <i>et al.</i> (2020) [22]	WideResNet-70-16	31.89	32.07	33.70	33.94 (5)	33.72	<u>33.92</u>	+1.85
11	Rebuffi <i>et al.</i> (2021) [37]	WideResNet-70-16	30.45	30.72	32.75	<u>33.06</u> (6)	32.79	33.10	+2.38
Average Rank			5.92	4.92	2.79	2.00	3.50	1.58	
ImageNet ($\epsilon = 4/255$)									
12	Salman <i>et al.</i> (2020) [39]	ResNet-18	70.60	70.74	73.72	<u>74.38</u> (5)	74.24	74.52	+3.87
13	Salman <i>et al.</i> (2020) [39]	ResNet-50	61.38	61.58	63.70	<u>64.92</u> (7)	64.5	64.94	+3.36
14	Wong <i>et al.</i> (2020) [49]	ResNet-50	70.28	70.46	71.94	73.20 (5)	72.96	<u>73.10</u>	+2.64
15	Engstrom <i>et al.</i> (2019) [17]	ResNet-50	67.62	67.82	68.60	70.12 (5)	69.86	<u>69.92</u>	+2.10
16	Salman <i>et al.</i> (2020) [39]	WideResNet-50-2	59.02	59.12	59.92	61.26 (5)	60.76	<u>61.14</u>	+2.02
Average Rank			6.00	5.00	4.00	1.40	3.00	1.60	

[†]: reported results from the paper [51], with attack step $N_{\text{iter}} = 100$.

Determining Loss Synergistic Patterns. For every dominant perturbation δ^* , we check its contribution to the loss functions. In particular, for each perturbation δ^* , if its i -th loss value $\tilde{f}_i(\delta^*) > C * \max_{\delta \in \Delta} \tilde{f}_i(\delta)$, we consider it as a contribution to the i -th loss function. Thus, for every dominant perturbation, we can get a contribution combination, which we call a loss synergistic pattern. We can record the loss synergistic pattern for each dominant perturbation across the dataset to facilitate the analysis of coupling effects between loss functions.

4.3. Implementation: Loss Functions

The final step of implementing our attack is to specify multiple surrogate loss functions. We incorporate a selection of significant loss functions that are well-documented in existing literature [10, 34, 46], along with innovative loss functions that have been identified through rigorous exploration in the domain of loss search [30, 50]. Details of these loss functions can be found in Table 1 and Table 2.

5. Experiment

5.1. Experiment Setup

Datasets and Models. We employed 17 distinct from RobustBench [12], which includes 12 models [4, 27, 36, 37, 40, 47] trained on the CIFAR-10 [28] dataset and 5 models [39, 49] based on ImageNet [15] dataset. For performance evaluation, we used all 10,000 test images from the CIFAR-10 validation dataset and 5,000 images from ImageNet validation dataset. To enable direct comparison with the reported accuracy of the ACG attack, we preserved the same image indexing for the ImageNet dataset as [51].

Comparative Attacks. For comparative purposes, we incorporate the widely recognized APGD-CE attack, the state-of-the-art ACG-CW, and the comprehensive APGD-All attack. The latter aggregates optimal outcomes from an ensemble of eight distinct APGD attacks, each employing unique loss functions from Table 1.

Attack Parameters. Notably, the number of iterations for our implemented attacks, including MOS Attack, APGD-CE, and APGD-All, are uniformly set to 50. This choice ensures thorough and rigorous testing of all methods. Ad-

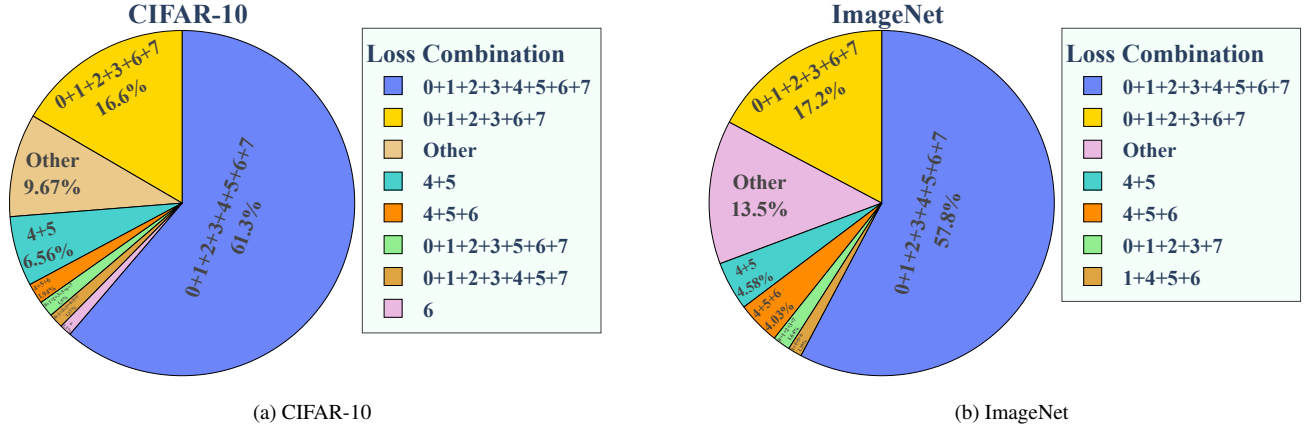


Figure 2. Occurrences of different loss synergistic patterns across CIFAR-10 and ImageNet datasets. We only retain the top patterns that account for more than 1% of the adversarial examples.

ditionally, the remaining attack parameters follow the same configuration as outlined in APGD [11].

5.2. Overall Results

This section presents the comparative results of our proposed MOS-8 attack alongside other competing algorithms, delineating them in terms of Attack Success Rate (ASR). Detailed outcomes are provided in Table Table 3.

Single-objective v.s. Multi-objective. The results demonstrate that multi-objective approaches outperform single-objective approaches. The most effective single-objective approach is the ACG-CW attack, utilizing 5 restarts and 100 attack steps; however, despite a considerably higher number of attack steps $N_{\text{iter}} = 100$, it only achieved the best ASR in 3 out of 17 instances, with a rate of 3 out of 12 for CIFAR-10 and failing to succeed in any of the 5 cases for ImageNet.

MOS-8 v.s. APGD-All. The MOS-8 Attack demonstrates a slight superiority over APGD-All. Notably, the MOS-8 Attack achieved comparable or better results with only five adversarial examples, whereas APGD-All utilized eight. MOS-8 Attack achieved an average rank of 1.58 on CIFAR-10 and 1.60 on ImageNet, while APGD-All attained an average rank of 2.00 on CIFAR-10 and 1.40 on ImageNet.

Loss Functions. APGD-All’s findings underscored the superiority of loss 4-7 in Table 1, as attacks using them consistently achieved the highest ASR out of 8 attack across all models on both CIFAR-10 and ImageNet. This observation reveals the importance of selecting appropriate loss functions for adversarial attacks.

Model Robutness. As the complexity of the model escalates, mirrored by the sophistication of the architecture, the performance disparity between MOS-8 Attack and APGD-CE narrows. This indicates an incremental trend of model robustness, making them more challenging to be attacked.

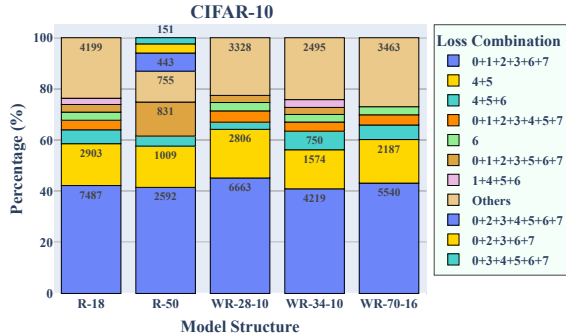
Table 4. A marked discrepancy from the theoretical upper bound of set-based optimization, as estimated by comprehensive attacks.

ID	Architecture	MOS-8 (1)	MOS-8 (8)	Upper Bound	Diff.
0	R-18	42.59	42.84	42.92	-0.33/-0.08
1	R-18	42.03	42.21	42.37	-0.34/-0.16
2	R-18	43.79	44.18	44.40	-0.61/-0.22
3	R-50	48.09	48.22	48.36	-0.27/-0.14
4	WR-28-10	36.77	36.96	37.17	-0.40/-0.21
5	WR-28-10	32.25	32.47	32.67	-0.42/-0.30
6	WR-28-10	38.91	39.12	39.26	-0.35/-0.14
7	WR-34-10	38.97	39.39	39.73	-0.76/-0.34
8	WR-34-10	36.69	36.95	37.16	-0.47/-0.21
9	WR-70-16	33.33	33.52	33.82	-0.49/0.30
10	WR-70-16	33.72	33.95	34.12	-0.40/-0.17
11	WR-70-16	32.79	33.08	33.32	-0.53/-0.24

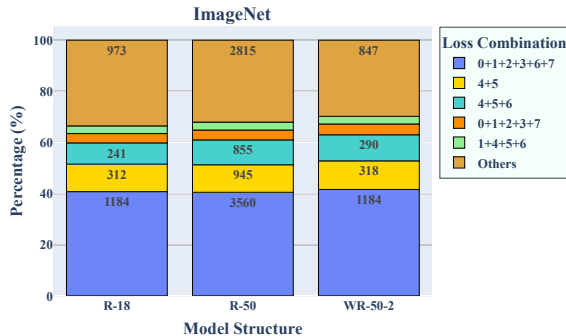
5.3. MOS Attack Upper Bound

To evaluate the gap between the performance of our adversarial examples and the hypothetical optimal set delineated in Section 3.3, we conducted an array of APGD attacks on CIFAR-10 dataset. Specifically, we implemented 8 separate APGD attacks, each employing a unique loss function and accompanied by five restarts. For each image in the dataset, we identified the single most effective adversarial example out of the 40 (8 attacks x 5 restarts) created. The ASR was then calculated based on these examples to serve as an indicator of the maximum achievable performance.

Results. The comparison between the MOS-8 Attack with $K = 1$, $K = 8$, and the upper bound is presented in Table 4. Generally, the discrepancy is minimal. Even when a single adversarial example is tailored to address all loss functions in MOS-8 Attack, near-optimal outcomes are achieved. Additionally, leveraging eight adversarial examples brings the results within a negligible difference from the upper bound, with less than a 0.35% gap in ASR.



(a) CIFAR-10



(b) ImageNet

Figure 3. Detailed distribution of loss synergistic patterns across different model architectures. We only retain the top patterns that account for more than 1% of the adversarial examples.

5.4. MOS Attack Analysis.

In this section, we employ our framework to conduct an automated analysis of the relationships among various loss functions. The solutions used for analysis is obtained from MOS-8 Attack with $K = 8$ for both CIFAR-10 and ImageNet datasets. The parameters selected were a sparsity coefficient of $\lambda = 1$, a binary threshold of $T = 0.85$, and a contribution threshold of $C = 0.75$.

We start by identifying the synergistic patterns among loss functions for all model architectures within each dataset. Subsequently, informed by these patterns, we design the MOS-3* attack, utilizing three selected surrogate loss functions.

5.4.1 Loss Synergistic Pattern

Figure 2 depicts the synergistic loss patterns for CIFAR-10 and ImageNet. A significant portion of the adversarial examples—61.3% for CIFAR-10 and 57.8% for ImageNet—contribute to all loss functions, indicating that the majority of solutions optimize them concurrently. This observation suggests a low level of conflict among the loss functions and helps explain why employing a single loss function ($K = 1$) can yield near-optimal results.

Table 5. The comparative results of MOS-3* Attack and MOS-3 Attack, with reference results from MOS-8 Attack.

CIFAR-10 ($\epsilon = 8/255$)						
ID	All (1)*8	MOS-8 (5)	MOS-3 (1)	MOS-3 (3)	MOS-3* (1)	MOS-3* (3)
9	33.50 (5)	<u>33.51</u>	31.19	31.47	<u>33.51</u>	33.60
10	33.94 (5)	33.92	31.63	31.83	33.91	<u>33.93</u>
11	33.06 (6)	33.10	30.23	30.43	33.03	<u>33.07</u>
ImageNet ($\epsilon = 4/255$)						
16	61.26 (5)	<u>61.14</u>	58.82	59.24	60.86	61.08

Transferability of Synergistic Patterns. We extended our analysis to the transferability of these patterns across different model architectures. We removed the common pattern containing all the losses and plotted the pattern distributions for each model architecture. As depicted in Figure 3, the patterns demonstrate stability across datasets and models, with a minor exception observed in ResNet-50’s patterns for the CIFAR-10 dataset, which exhibited some unique, less common patterns.

5.4.2 MOS-3* Attack

The predominant patterns are **0+1+2+3+6+7** and **4+5**, as they ranked first and second in both datasets, as shown in Figure 3. We subsequently constructed a compact version of MOS Attack, termed MOS-3* Attack, using losses 5, 6, and 7. For validation of the effectiveness of MOS-3* Attack, we compared it against MOS-3 Attack, which is constructed utilizing the first three loss functions.

Results. As illustrated in Table 5, MOS-3* Attack outperforms MOS-3 Attack. MOS-3* Attack has achieved better performance across all models with $K = 1$ adversarial example, surpassing that of MOS-3 Attack with $K = 3$ adversarial examples. Moreover, MOS-3* Attack’s performance is comparable to that of MOS-8 Attack. The above outcomes confirm the value of leveraging loss synergistic patterns to design more efficient yet effective attacks.

6. Conclusion

Our work has introduced the MOS Attack, a novel multi-objective adversarial attack framework that effectively combines multiple surrogate loss functions to generate adversarial examples. The MOS-8 Attack, utilizing eight such functions, has shown superior performance on CIFAR-10 and ImageNet datasets compared to existing state-of-the-art methods. The framework’s automated method for identifying synergistic patterns among loss functions has led to the development of the efficient MOS-3* tri-objective attack. Our contributions offer a scalable and extensible approach to adversarial machine learning, highlighting the potential for more resource-efficient and potent adversarial attack strategies in the future.

References

- [1] Maksym Andriushchenko, Francesco Croce, Nicolas Flammarion, and Matthias Hein. Square attack: A query-efficient black-box adversarial attack via random search. In *Computer Vision - ECCV 2020 - 16th European Conference*. Springer, 2020. 2
- [2] Nikolaos Antoniou, Efthymios Georgiou, and Alexandros Potamianos. Alternating objectives generates stronger pgd-based adversarial attacks. *CoRR*, 2022. 1, 2
- [3] Sanjeev Arora, László Babai, Jacques Stern, and Z. Sweedyk. The hardness of approximate optima in lattices, codes, and systems of linear equations. *J. Comput. Syst. Sci.*, 1997. 1
- [4] Maximilian Augustin, Alexander Meinke, and Matthias Hein. Adversarial robustness on in- and out-distribution improves explainability. In *Computer Vision - ECCV 2020 - 16th European Conference*. Springer, 2020. 6
- [5] Alina Elena Baia, Gabriele Di Bari, and Valentina Poggioni. Effective universal unrestricted adversarial attacks using a MOE approach. In *Applications of Evolutionary Computation - 24th International Conference, EvoApplications*. Springer, 2021. 2
- [6] Amir Beck and Marc Teboulle. Smoothing and first order methods: A unified framework. *SIAM J. Optim.*, 2012. 4
- [7] Yulong Cao, Chaowei Xiao, Benjamin Cyr, Yimeng Zhou, Won Park, Sara Rampazzi, Qi Alfred Chen, Kevin Fu, and Z. Morley Mao. Adversarial sensor attack on lidar-based perception in autonomous driving. In *Proceedings of the 2019 ACM SIGSAC Conference on Computer and Communications Security, (CCS)*. ACM, 2019. 1
- [8] Nicholas Carlini and David A. Wagner. Towards evaluating the robustness of neural networks. In *2017 IEEE Symposium on Security and Privacy, SP*. IEEE Computer Society, 2017. 1, 2, 5
- [9] Tianlong Chen, Sijia Liu, Shiyu Chang, Yu Cheng, Lisa Amini, and Zhangyang Wang. Adversarial robustness: From self-supervised pre-training to fine-tuning. In *2020 IEEE/CVF Conference on Computer Vision and Pattern Recognition, CVPR 2020, Seattle, WA, USA, June 13-19, 2020*. Computer Vision Foundation / IEEE, 2020. 6
- [10] Francesco Croce and Matthias Hein. Minimally distorted adversarial examples with a fast adaptive boundary attack. In *Proceedings of the 37th International Conference on Machine Learning, ICML, 2020*. 5, 6
- [11] Francesco Croce and Matthias Hein. Reliable evaluation of adversarial robustness with an ensemble of diverse parameter-free attacks. In *Proceedings of the 37th International Conference on Machine Learning, ICML*. PMLR, 2020. 1, 2, 3, 4, 5, 7
- [12] Francesco Croce, Maksym Andriushchenko, Vikash Sehswag, Edoardo DeBenedetti, Nicolas Flammarion, Mung Chiang, Prateek Mittal, and Matthias Hein. Robustbench: a standardized adversarial robustness benchmark. In *Proceedings of the Neural Information Processing Systems Track on Datasets and Benchmarks 1, NeurIPS Datasets and Benchmarks*, 2021. 6
- [13] Kalyanmoy Deb, Samir Agrawal, Amrit Pratap, and T. Meyarivan. A fast and elitist multiobjective genetic algorithm: NSGA-II. *IEEE Trans. Evol. Comput.*, 2002. 3
- [14] Timo M. Deist, Monika Grewal, Frank J. W. M. Dankers, Tanja Alderliesten, and Peter A. N. Bosman. Multi-objective learning using HV maximization. In *Evolutionary Multi-Criterion Optimization - 12th International Conference, EMO*. Springer, 2023. 2
- [15] Jia Deng, Wei Dong, Richard Socher, Li-Jia Li, Kai Li, and Li Fei-Fei. Imagenet: A large-scale hierarchical image database. In *2009 IEEE Computer Society Conference on Computer Vision and Pattern Recognition CVPR*. IEEE Computer Society, 2009. 1, 2, 6
- [16] Yinpeng Dong, Hang Su, Baoyuan Wu, Zhifeng Li, Wei Liu, Tong Zhang, and Jun Zhu. Efficient decision-based black-box adversarial attacks on face recognition. In *IEEE Conference on Computer Vision and Pattern Recognition, (CVPR)*. Computer Vision Foundation / IEEE, 2019. 1
- [17] Logan Engstrom, Andrew Ilyas, Hadi Salman, Shibani Santurkar, and Dimitris Tsipras. Robustness (python library), 2019. 6
- [18] Qi-An Fu, Yinpeng Dong, Hang Su, Jun Zhu, and Chao Zhang. Autoda: Automated decision-based iterative adversarial attacks. In *31st USENIX Security Symposium, USENIX Security*. USENIX Association, 2022. 2
- [19] Narmin Ghaffari Laleh, Daniel Truhn, Gregory Patrick Veldhuizen, Tianyu Han, Marko van Treeck, Roman D Buelow, Rupert Langer, Bastian Dislich, Peter Boor, Volkmar Schulz, et al. Adversarial attacks and adversarial robustness in computational pathology. *Nature communications*, 2022. 1
- [20] Ian J. Goodfellow, Jonathon Shlens, and Christian Szegedy. Explaining and harnessing adversarial examples. In *3rd International Conference on Learning Representations, ICLR, 2015*. 1, 2, 5
- [21] Sven Gowal, Jonathan Uesato, Chongli Qin, Po-Sen Huang, Timothy A. Mann, and Pushmeet Kohli. An alternative surrogate loss for pgd-based adversarial testing. *CoRR*, 2019. 1, 2, 5
- [22] Sven Gowal, Chongli Qin, Jonathan Uesato, Timothy A. Mann, and Pushmeet Kohli. Uncovering the limits of adversarial training against norm-bounded adversarial examples. *CoRR*, abs/2010.03593, 2020. 6
- [23] Sven Gowal, Sylvestre-Alvise Rebuffi, Olivia Wiles, Florian Stimberg, Dan Andrei Calian, and Timothy A. Mann. Improving robustness using generated data. In *Advances in Neural Information Processing Systems 34: Annual Conference on Neural Information Processing Systems 2021, NeurIPS, 2021*. 6
- [24] Ping Guo, Cheng Gong, Xi Lin, Zhiyuan Yang, and Qingfu Zhang. Exploring the adversarial frontier: Quantifying robustness via adversarial hypervolume. *arXiv preprint arXiv:2403.05100*, 2024. 2
- [25] Ping Guo, Fei Liu, Xi Lin, Qingchuan Zhao, and Qingfu Zhang. L-autoda: Large language models for automatically evolving decision-based adversarial attacks. In *Proceedings of the Genetic and Evolutionary Computation Conference Companion, GECCO*. ACM, 2024. 2

- [26] Kaiming He, Xiangyu Zhang, Shaoqing Ren, and Jian Sun. Deep residual learning for image recognition. In *IEEE Conference on Computer Vision and Pattern Recognition, CVPR*. IEEE Computer Society, 2016. 1
- [27] Hanxun Huang, Yisen Wang, Sarah M. Erfani, Quanquan Gu, James Bailey, and Xingjun Ma. Exploring architectural ingredients of adversarially robust deep neural networks. In *Advances in Neural Information Processing Systems 34: Annual Conference on Neural Information Processing Systems 2021, (NeurIPS)*, 2021. 6
- [28] A. Krizhevsky. Learning Multiple Layers of Features from Tiny Images. Technical report, Univ. Toronto, 2009. 1, 2, 6
- [29] Alexey Kurakin, Ian J. Goodfellow, and Samy Bengio. Adversarial examples in the physical world. In *5th International Conference on Learning Representations, ICLR*, 2017. 5
- [30] Hao Li, Tianwen Fu, Jifeng Dai, Hongsheng Li, Gao Huang, and Xizhou Zhu. Autoloss-zero: Searching loss functions from scratch for generic tasks. In *IEEE/CVF Conference on Computer Vision and Pattern Recognition, CVPR*. IEEE, 2022. 1, 2, 6
- [31] Xi Lin, Yilu Liu, Xiaoyuan Zhang, Fei Liu, Zhenkun Wang, and Qingfu Zhang. Few for many: Tchebycheff set scalarization for many-objective optimization. *CoRR*, 2024. 4, 5
- [32] Xi Lin, Xiaoyuan Zhang, Zhiyuan Yang, Fei Liu, Zhenkun Wang, and Qingfu Zhang. Smooth tchebycheff scalarization for multi-objective optimization. In *Forty-first International Conference on Machine Learning, ICML*, 2024. 4
- [33] Shengcai Liu, Ning Lu, Wenjing Hong, Chao Qian, and Ke Tang. Effective and imperceptible adversarial textual attack via multi-objectivization. *ACM Trans. Evol. Learn. Optim.*, 2024. 2
- [34] Aleksander Madry, Aleksandar Makelov, Ludwig Schmidt, Dimitris Tsipras, and Adrian Vladu. Towards deep learning models resistant to adversarial attacks. In *6th International Conference on Learning Representations, ICLR*, 2018. 1, 2, 3, 5, 6
- [35] Kaisa Miettinen. *Nonlinear multiobjective optimization*. Springer Science & Business Media, 2012. 3
- [36] Rahul Rade and Seyed-Mohsen Moosavi-Dezfooli. Reducing excessive margin to achieve a better accuracy vs. robustness trade-off. In *The Tenth International Conference on Learning Representations, (ICLR)*. OpenReview.net, 2022. 6
- [37] Sylvestre-Alvise Rebuffi, Sven Gowal, Dan A. Calian, Florian Stimberg, Olivia Wiles, and Timothy A. Mann. Fixing data augmentation to improve adversarial robustness. *CoRR*, 2021. 6
- [38] Sara Sabour, Nicholas Frosst, and Geoffrey E. Hinton. Dynamic routing between capsules. In *Advances in Neural Information Processing Systems 30: Annual Conference on Neural Information Processing Systems*, 2017. 1
- [39] Hadi Salman, Andrew Ilyas, Logan Engstrom, Ashish Kapoor, and Aleksander Madry. Do adversarially robust imagenet models transfer better? In *Advances in Neural Information Processing Systems 33: Annual Conference on Neural Information Processing Systems 2020, NeurIPS*, 2020. 6
- [40] Vikash Sehwal, Saeed Mahloujifar, Tinashe Handina, Sihui Dai, Chong Xiang, Mung Chiang, and Prateek Mittal. Robust learning meets generative models: Can proxy distributions improve adversarial robustness? In *The Tenth International Conference on Learning Representations, (ICLR)*. OpenReview.net, 2022. 6
- [41] Gaurang Sriramanan, Sravanti Addepalli, Arya Baburaj, and Venkatesh Babu R. Guided adversarial attack for evaluating and enhancing adversarial defenses. In *Advances in Neural Information Processing Systems 33: Annual Conference on Neural Information Processing Systems 2020, NeurIPS*, 2020. 1, 2, 5
- [42] Takahiro Suzuki, Shingo Takeshita, and Satoshi Ono. Adversarial example generation using evolutionary multi-objective optimization. In *IEEE Congress on Evolutionary Computation, CEC*. IEEE, 2019. 2
- [43] Christian Szegedy, Wojciech Zaremba, Ilya Sutskever, Joan Bruna, Dumitru Erhan, Ian J. Goodfellow, and Rob Fergus. Intriguing properties of neural networks. In *2nd International Conference on Learning Representations, ICLR*, 2014. 1, 5
- [44] Hanrui Wang, Shuo Wang, Cunjian Chen, Massimo Tistarelli, and Zhe Jin. A multi-task adversarial attack against face authentication. *CoRR*, 2024. 2
- [45] Rui Wang, Qingfu Zhang, and Tao Zhang. Pareto adaptive scalarising functions for decomposition based algorithms. In *Evolutionary Multi-Criterion Optimization - 8th International Conference, EMO*. Springer, 2015. 3
- [46] Yisen Wang, Difan Zou, Jinfeng Yi, James Bailey, Xingjun Ma, and Quanquan Gu. Improving adversarial robustness requires revisiting misclassified examples. In *8th International Conference on Learning Representations, ICLR*. OpenReview.net, 2020. 1, 2, 5, 6
- [47] Zekai Wang, Tianyu Pang, Chao Du, Min Lin, Weiwei Liu, and Shuicheng Yan. Better diffusion models further improve adversarial training. In *International Conference on Machine Learning, (ICML)*. PMLR, 2023. 6
- [48] Phoenix Neale Williams and Ke Li. Black-box sparse adversarial attack via multi-objective optimisation CVPR proceedings. In *IEEE/CVF Conference on Computer Vision and Pattern Recognition, CVPR*. IEEE, 2023. 2
- [49] Eric Wong, Leslie Rice, and J. Zico Kolter. Fast is better than free: Revisiting adversarial training. In *8th International Conference on Learning Representations, ICLR*. OpenReview.net, 2020. 6
- [50] Pengfei Xia, Ziqiang Li, and Bin Li. Tightening the approximation error of adversarial risk with auto loss function search. In *Proceedings of the Genetic and Evolutionary Computation Conference Companion, GECCO 2024, Melbourne, VIC, Australia, July 14-18, 2024*, 2024. 2, 5, 6
- [51] Keiichiro Yamamura, Haruki Sato, Nariaki Tateiwa, Nozomi Hata, Toru Mitsutake, Issa Oe, Hiroki Ishikura, and Katsuki Fujisawa. Diversified adversarial attacks based on conjugate gradient method. In *International Conference on Machine Learning, ICML*. PMLR, 2022. 1, 2, 3, 6
- [52] Hongyang Zhang, Yaodong Yu, Jiantao Jiao, Eric P. Xing, Laurent El Ghaoui, and Michael I. Jordan. Theoretically

principled trade-off between robustness and accuracy. In *Proceedings of the 36th International Conference on Machine Learning, ICML*. PMLR, 2019. 1

- [53] Qingfu Zhang and Hui Li. MOEA/D: A multiobjective evolutionary algorithm based on decomposition. *IEEE Trans. Evol. Comput.*, 2007. 3